Macroapproach kinetics of ethanol fermentation by *Saccharomyces cerevisiae:* experimental studies and mathematical modelling

Maciej Starzak*
Department of Chemical Engineering, University of Natal, King George V Avenue, 4001 Durban (South Africa)

Liliana Krzystek, Lech Nowicki and Henryk Michalski
Bioprocess Engineering Section, Faculty of Process and Environmental Engineering, Technical University of Łódź, Wólczańska 175, 90-924 Łódź (Poland)

(Received September 27, 1993; in final form January 4, 1994)

Abstract

The kinetics of ethanol fermentation by *Saccharomyces cerevisiae* was studied both experimentally and theoretically. Batch fermentations were performed anaerobically on synthetic media with an initial sucrose content of 130–210 g dm^{-3} under both controlled and uncontrolled pH conditions. A series of ten unstructured models involving microbial growth, substrate utilization and ethanol formation were applied to the data. The models were based on a formal macroapproach and either Pirt's or Herbert's concept of microbial energetics. The model giving the best fit to experimental data at constant pH satisfied Herbert's concept of endogenous metabolism and included an exponential term responsible for the effect of ethanol inhibition on the growth rate. A correction factor was introduced to account for the effect of pH on the biomass growth rate in fermentations with no pH control. A linear relationship between hydrogen ion consumption rate and growth rate was assumed and confirmed experimentally. Finally, it is shown that models identified exclusively by fitting the concentration data might result in a very poor estimate of the ethanol yield coefficient $Y_{P/S}$ at varying growth rates. In order to make the kinetic equations stoichiometrically consistent and hence to have an idea of what type of constraint should be used for the purpose of parameter estimation, a biochemically structured model based on the Roels approach was developed. Two parameter constraints, one resulting from fermentation stoichiometry and another from the yield function monotonicity, are proposed.

1. Introduction

Ethanol produced from cheap, renewable resources can compensate for the shortage of fossil fuels in some branches of the economy. Renewable materials such as molasses, starch, agricultural raw materials, cellulose wastes, and some municipal and industrial waste water, can be used as a carbon source. Traditionally, various species of *Saccharomyces* yeasts are used for fermentation, although ethanol can be produced by *Kluyveromyces* and *Candida* yeasts as well. Recently, the industrial application of *Zymomonas* bacteria has also been extensively studied. An important research problem in this field is to study the kinetics of fermentation including microbial growth, substrate utilization and ethanol formation. The aim of this work is to discuss the applicability of different mathematical models for ethanol fermentation, as derived using macroapproach kinetics.

2. Macroapproach kinetics of ethanol fermentation

Ethanol fermentation is a typical example of a process in which utilization of the carbon source cannot be split into two processes, namely production of biomass and formation of product. Ethanol is the end product of energy metabolism associated directly with biomass growth. It is, however, a strong inhibitor capable of retarding metabolic activity.

The majority of kinetic models describing microbial growth during ethanol fermentation use a formal macroapproach to bioprocessing [1]. They are empirical and based on either Monod's equation [2] or on its numerous modifications which take

*Author to whom correspondence should be addressed.

SSDI 0923-0467(94)00210-0

into account the inhibition of microbial growth by a high concentration of product and/or substrate. In many models proposed so far the effect of ethanol inhibition is explained via the mechanism of non-competitive inhibition of a simple reversible enzymatic reaction [3–5]. In the non-mechanistic approach, it is assumed that the inhibition by ethanol follows a linear [6–13], power [14–18], exponential [19–21], hyperbolic [22] or another non-linear formula [23–26]. The kinetics of inhibition due to a high substrate concentration depends on the type of substrate and micro-organism. It is usually described by an exponential [12, 20] or hyperbolic dependence [8–10, 12, 24]. In processes involving a high concentration of microbial cells, the biomass itself also inhibits growth and product formation [11, 14, 18, 21]. This is quite well represented by a term proportional to the biomass concentration [21].

In order to describe the substrate utilization rate in ethanol fermentations, the relation proposed by Herbert [27] has been used in numerous studies [7–9, 11, 14, 17, 19, 20, 24], whereas the rate of substrate consumption defined by Pirt's formula [28] is rarely applied [21]. Only a few authors assume that there is a term responsible for the substrate consumption for building up the product [21, 22].

Equations describing the rate of product formation often have a form analogous to that representing the specific growth rate [7–9, 11, 19–21]. Mathematically equivalent formulae resulting from Herbert's [27] and Pirt's [28] concepts or given by the Luedeking–Piret law [22, 29, 30] are also used.

A different approach to ethanol fermentation kinetics, in which the rates of biomass and ethanol formation and substrate utilization are described in terms of formal chemical reaction kinetics, is presented in refs. 31–33. The solution of these models has been made possible by the wide application of computer techniques for the identification of complex kinetic systems.

Another group of kinetic models, based on biochemically structured balances of microbial metabolism, has been proposed by Roels and coworkers [34–36]. In this approach, the complex machinery of cellular processes has been arranged into some fundamental types of reaction patterns: catabolic pathways (breakdown of substrates into energy and small molecules), anabolic pathways (synthesis of precursors for biomass), polymerization of the precursors to biomass, and the maintenance metabolism keeping the cellular machinery operative. A list of the most important metabolic processes accompanying ethanol fermentation with sucrose as a carbon source is shown in Table 1. Roels proposed a semi-theoretical model of ethanol production assuming strictly anaerobic conditions for the process [35, 36]. Some of the reactions listed in Table 1, such as synthesis of biomass precursors (I), production of ethanol (III), formation of glycerol (IV), polymerization of biomass precursors (XI) and maintenance processes (XII) have been added to his kinetic model (based on glucose as the carbon source). The formation of any other by-products of ethanol fermentation, for example acetaldehyde, organic acids and butanediol [38], was assumed to be negligible. As a result, the rate equations for substrate consumption and product formation could be derived after applying a quasi-steady-state approximation (QSSA) to biomass precursors, energy carriers (ATP, GTP) and reducing equivalents ($NADH_2$, $NADPH_2$ $FADH_2$). Although the final mathematical form of the Roels model turned out to be the same as that of well known empirical models based on Pirt's concept and the Luedeking–Piret law, a great advantage of this model is the fact that it immediately imposes stoichiometric constraints on the rates of substrate consumption and product formation.

Changes in pH of the fermentation medium significantly affect process parameters. Theoretical studies to determine the effect of pH on the course of fermentation encounter serious difficulties because the mechanism of the action of free hydrogen and hydroxyl ions on the activity, growth and multiplication of micro-organisms is not well specified [39]. Curves illustrating the dependence of population growth rate on pH of the medium are usually characterized by a flat maximum, so that there is some pH range in which the growth rate is subject to slight changes only. The location of this maximum on the pH axis depends on the nature of the process. In ethanol fermentation, the optimum pH range is 4 to 6 [40, 41]. The addition of the pH effect to the growth rate equation can take several forms, as reviewed by Andreyeva and Biryukov [39]. Commonly, they are various modifications of well known relationships expressing the growth rate of micro-organisms.

The inhibition of cellular metabolism at elevated levels of dissolved carbon dioxide is widely recognized [42]. Some studies have been carried out to determine the influence of CO_2 on the fermentation of ethanol at moderate and high CO_2 pressures (up to 7 MPa). It was found, however, that ethanol production was unaffected by pressures below 0.5 MPa [43, 44]. In this work the partial pressure of CO_2 did not exceed 0.1 MPa and was approximately constant, hence the effect of CO_2 could be ignored.

TABLE 1. Stoichiometry of main metabolic pathways appearing in the ethanol fermentation by *Saccharomyces cerevisiae* on sucrose

I	Formation of biomass precursors from sucrose (anabolism) $1.095CH_{11/6}O_{11/12} + 0.15NH_3 + 0.051ATP \longrightarrow CH_{1.61}O_{0.52}N_{0.15} + 0.13'H_2' + 0.095CO_2 + 0.294H_2O$
II	Formation of biomass precursors from ethanol (anabolism) $1.285CH_3O_{0.5} + 0.15NH_3 + 1.588ATP + 0.448H_2O \longrightarrow CH_{1.61}O_{0.52}N_{0.15} + 1.795'H_2' + 0.285CO_2$
III	Fermentation of sucrose to ethanol $1.5CH_{11/6}O_{11/12} + 0.125H_2O \longrightarrow CH_3O_{0.5} + 0.5CO_2 + 0.5ATP$
IV	Formation of glycerol $CH_{11/6}O_{11/12} + 1/12H_2O + 1/3ATP + 1/3'H_2' \longrightarrow CH_{8/3}O$
V	Formation of acetaldehyde $1.5CH_{11/6}O_{11/12} + 0.125H_2O \longrightarrow CH_2O_{0.5} + 0.5CO_2 + 0.5ATP + 0.5'H_2'$
VI	Formation of acetic acid $1.5CH_{11/6}O_{11/12} + 0.625H_2O \longrightarrow CH_2O + 0.5CO_2 + 0.5ATP + 'H_2'$
VII	Formation of butanediol $1.5CH_{11/6}O_{11/12} + 0.125H_2O \longrightarrow CH_{2.5}O_{0.5} + 0.5CO_2 + 0.5ATP + 0.25'H_2'$
VIII	Catabolism of sucrose* $CH_{11/6}O_{11/12} + 13/12H_2O \longrightarrow CO_2 + 2/3ATP + 2'H_2'$
IX	Catabolism of ethanol* $CH_3O_{0.5} + 0.5ATP + 1.5H_2O \longrightarrow CO_2 + 3'H_2'$
X	Oxidative phosphorylation* $0.5O_2 + 'H_2' \longrightarrow H_2O + \delta ATP$
XI	Polymerization of biomass precursors $CH_{1.61}O_{0.52}N_{0.15} + \kappa ATP \longrightarrow$ Biomass
XII	Consumption of ATP in maintenance processes

For the sake of clarity, ADP, P_i (inorganic phosphate) and water involved in phosphorylations and dephosphorylations are omitted in the stoichiometry.

The symbol 'H_2' represents reducing equivalents.

Stoichiometries of reactions I and II were adjusted to sucrose as a carbon source using the data for glucose from Oura [37].

Reactions marked by an asterisk require aerobic conditions.

$CH_{1.61}O_{0.52}N_{0.15}$ is the elemental composition formula of ash-free yeast [37]; the elemental composition formulae per one carbon were used for other carbon compounds.

δ is the efficiency of oxidative phosphorylation [36].

κ is the specific ATP demand in the polymerization of one C-mole of biomass from precursors.

3. Experimental conditions

The yeast strain used in this study was *Saccharomyces cerevisiae* hybrid G-67, provided by the Institute of Microbiology, the USSR Academy of Sciences, Moscow. The culture was maintained on agar slants containing malt extract (3 g dm^{-3}), yeast extract (3 g dm^{-3}), peptone (5 g dm^{-3}), glucose (10 g dm^{-3}), agar (20 g dm^{-3}) and distilled water. The slants were stored at 4 °C. The cultivation medium contained 130–210 g dm^{-3} sucrose, 3.0 g dm^{-3} $(NH_4)_2SO_4$, 0.7 g dm^{-3} $MgSO_4$, 0.5 g dm^{-3} NaCl, 1.0 g dm^{-3} KH_2PO_4, 0.1 g dm^{-3} K_2HPO_4 and 0.2% yeast extract. Inocula for fermentation were prepared in shake flasks containing pre-sterilized cultivation medium held at 30 °C for 24 h. The volume of inoculum was calculated to be 5% of the total culture volume. Experimental runs were performed in a laboratory fermentor of 1.5 dm^3 working volume. The fermentor was equipped with standard control instrumentation (temperature, pH, stirrer speed) and was agitated by a turbine type stirrer. It was also fitted with a CO_2 exhaustion port and an aseptic sampling system. The whole apparatus was sterilized by autoclaving.

Experimental studies involved four batch fermentation runs performed at atmospheric pressure, constant temperature ($T = 30 \pm 0.1$ °C) and agitation ($n = 500$ rev min^{-1}) under anaerobic conditions. The first two runs were performed under pH control at the constant value of 5.8. The pH level was regulated by 1.0 N NaOH. The next two runs were carried out without pH control. Under these conditions the pH decreased from an initial value of 5.8 to 2.0.

The following assays were made: cell concentration on a spectrophotometer by correlating cell dry weight with optical density (OD) at 620 nm; sugar content by the anthrone reagent method [45]; ethanol concentration by a refractometric method after standard distillation. The viability of cells was measured indirectly by staining the cells with methylene blue on a microscope slide.

4. Identification of kinetic models

All the kinetic models of cellular metabolism which are discussed in this paper can be classified as unstructured. The kinetic model of ethanol biosynthesis comprises equations representing the rate of biomass growth r_X, the sucrose consumption rate r_S, the ethanol production rate r_P and eventually the rate of hydrogen ion formation r_H. Since all the experimental runs were performed in a batch fermentor, the following material balances describing the process can be written (see Appendix A):

$$\frac{dX}{dt} = r_X \qquad X(0) = X_0 \tag{1}$$

$$\frac{dS}{dt} = r_S \qquad S(0) = S_0 \tag{2}$$

$$\frac{dP}{dt} = r_P \qquad P(0) = P_0 \tag{3}$$

The initial conditions X_0, S_0 and P_0 are given in Table 2. They were not subject to the identification procedure but were taken directly from the measurements.

In order to estimate model parameters, the optimization technique originally developed by Levenberg [46] and Marquardt [47], and later applied to microbial kinetics by Nihtila and coworkers [48, 49], was employed. The performance index was defined as a measure of fitting experimental data for biomass, sucrose and ethanol:

$$J(\boldsymbol{k}) = \sum_{i=1}^{I} \sum_{j=1}^{N_i} \left\{ \left[\frac{X_{ij} - X_{ij}^*}{X_{max}} \right]^2 + \left[\frac{S_{ij} - S_{ij}^*}{S_{max}} \right]^2 + \left[\frac{P_{ij} - P_{ij}^*}{P_{max}} \right]^2 \right\} \tag{4}$$

The maximum experimental concentrations X_{max}, S_{max} and P_{max} appearing in eqn. (4) were taken as reference values. Differential equations of the initial-value problem (1–3) were integrated numerically using the Merson method [50]. In order to compare the applicability of different models of fermentation, the value of residual variance was used:

$$\sigma_R^2 = \frac{\min_{\mathbf{k}} J(\mathbf{k})}{\sum_{i=1}^{I} N_i - p} \tag{5}$$

The identification procedure was performed in two stages. In the first stage, models valid for constant pH were identified using relevant experimental data (pH 5.8). In the second stage, the models already identified were adopted to varying pH conditions.

TABLE 2. Initial concentrations (g dm^{-3}) in subsequent experimental runs

Run	X_0	S_0	P_0	$(pH)_{t=0}$
1	0.08	196	2.4	Constant (5.8)
2	0.09	129	0.8	Constant (5.8)
3	0.12	135	1.9	5.8
4	0.13	210	3.6	5.8

4.1. Models for constant pH conditions

The kinetics of ethanol fermentations performed at constant hydrogen ion concentrations are described by models 1–7 (see Table 3). These models contain from 4 to 12 parameters. Models 1–5 constitute the first group of kinetic models which have been developed under the assumption that the gross (observed) change in cell mass results from the growth process only, neglecting both endogenous metabolism and cell death [28]:

$$r_X = (r_X)_{growth} \tag{6}$$

In model 1 the biomass growth rate is described by the Monod equation [2]:

$$r_X = \frac{k_1 XS}{k_2 + S} \tag{7}$$

Additionally, it was assumed that the rates of substrate consumption and product formation are proportional to the rate of biomass growth (according to Monod's formulation of the biomass yield coefficient):

$$r_S = -k_3 r_X \tag{8}$$

$$r_P = k_4 r_X \tag{9}$$

A very high value of the residual variance ($\sigma_R^2 = 0.0364$) obtained in the identification calculations for model 1 confirms the well known fact that such simple kinetics are unsatisfactory. Large discrepancies between the experimental and model results (especially for biomass concentration) are shown in Figs. 1–3. As a consequence, the relationship describing the rate r_X has been modified in model 2 by adding an exponential term responsible for the effect of ethanol inhibition [19]:

$$r_X = \frac{k_1 XS}{k_2 + S} \exp(-k_5 P) \tag{10}$$

The residual variance obtained for model 2 was 0.0046. Such a significant improvement confirms the important role that product inhibition plays in

TABLE 3. Summary of mathematical models proposed for ethanol fermentation

Model	Characteristics	Parameters[a]	Rate equations
1	Substrate limitation (Monod type) No substrate and product inhibition r_S proportional to r_X r_P proportional to r_X Constant pH	$k_1 = 0.1594$ $k_2 = 44.98$ $k_3 = 28.60$ $k_4 = 8.173$	$r_X = \frac{k_1 XS}{k_2 + S}$ $r_S = -k_3 r_X$ $r_P = k_4 r_X$
2	Substrate limitation (Monod type) No substrate inhibition Ethanol inhibition (exponential) r_S proportional to r_X r_P proportional to r_X Realistic asymptotic behaviour Constant pH	$k_1 = 0.3386$ $k_2 = 7.260$ $k_3 = 18.29$ $k_4 = 7.877$ $k_5 = 0.0551$	$r_X = \frac{k_1 XS}{k_2 + S} \exp(-k_5 P)$ $r_S = -k_3 r_X$ $r_P = k_4 r_X$
3	Substrate limitation (Monod type) No substrate inhibition Ethanol inhibition (exponential) Pirt's concept of substrate utilization Luedeking–Piret law Unrealistic asymptotic behaviour Constant pH	$k_1 = 0.3916$ $k_2 = 20.01$ $k_3 = 10.85$ $k_4 = 4.000$ $k_5 = 0.0709$ $k_6 = 0.4541$ $k_7 = 0.2373$	$r_X = \frac{k_1 XS}{k_2 + S} \exp(-k_5 P)$ $r_S = -k_3 r_X - k_6 X$ $r_P = k_4 r_X + k_7 X$
4	Substrate limitation (Monod type) Substrate inhibition (competitive) Ethanol inhibition (exponential) Pirt's concept of substrate utilization Luedeking–Piret law Unrealistic asymptotic behaviour Constant pH	$k_1 = 0.3891$ $k_2 = 19.79$ $k_3 = 10.86$ $k_4 = 4.012$ $k_5 = 0.0708$ $k_6 = 0.4540$ $k_7 = 0.2368$ $k_8 \approx 0.0$	$r_X = \frac{k_1 XS}{k_2 + S + k_8 S^2} \exp(-k_5 P)$ $r_S = -k_3 r_X - k_6 X$ $r_P = k_4 r_X + k_7 X$
5	Substrate limitation (Monod type) No substrate inhibition Ethanol inhibition (hyperbolic) Pirt's concept of substrate utilization Luedeking–Piret law Unrealistic asymptotic behaviour Constant pH	$k_1 = 0.4607$ $k_2 = 25.52$ $k_3 = 10.87$ $k_4 = 3.977$ $k_5 = 0.0178$ $k_6 = 0.4542$ $k_7 = 0.2384$ $k_8 = 0.1027$	$r_X = \frac{k_1 XS}{k_2 + S} \frac{1 - k_5 P}{1 + k_8 P}$ $r_S = -k_3 r_X - k_6 X$ $r_P = k_4 r_X + k_7 X$
6	Substrate limitation (Monod type) No substrate inhibition Ethanol inhibition (exponential) Herbert's concept of endogenous metabolism r_S proportional to $(r_X)_{growth}$ r_P proportional to $(r_X)_{growth}$ Realistic asymptotic behaviour Constant pH	$k_1 = 0.3292$ $k_2 = 2.149$ $k_3 = 12.78$ $k_4 = 5.541$ $k_5 = 0.0454$ $k_6 = 0.0274$	$r_X = (r_X)_{growth} + (r_X)_{end}$ $r_S = -k_3 (r_X)_{growth}$ $r_P = k_4 (r_X)_{growth}$ $(r_X)_{growth} = \frac{k_1 XS}{k_2 + S} \exp(-k_5 P)$ $(r_X)_{end} = -k_6 X$
7	Formal chemical kinetics (power-type) Realistic asymptotic behaviour Constant pH	$k_1 = 0.0159$ $k_2 = 0.7607$ $k_3 = 0.7778$ $k_4 = -0.7234$ $k_5 = 0.0370$ $k_6 = 0.0920$ $k_7 = 0.6745$ $k_8 = 0.4249$ $k_9 = 0.9642$ $k_{10} = -0.1051$ $k_{11} = -0.1214$ $k_{12} = 0.3503$	$r_X = k_1 X^{k_2} S^{k_3} P^{k_4}$ $r_S = -k_5 X^{k_6} S^{k_7} P^{k_8}$ $r_P = k_9 X^{k_{10}} S^{k_{11}} P^{k_{12}}$

(continued)

TABLE 3. (*continued*)

Model	Characteristics	Parameters[a]	Rate equations
8	Substrate limitation (Monod type) No substrate inhibition Ethanol inhibition (exponential) Pirt's concept of substrate utilization Luedeking–Piret law Unrealistic asymptotic behaviour pH affected growth r_H proportional to r_X	k_1 to k_7 as in model 3 $k_9 = 2572$ $k_{10} = 8 \times 10^{-12}$ $k_{11} = 0.0023$	$r_X = \frac{k_1 XS}{k_2 F + S} \exp(-k_5 P)$ $F = \frac{1 + k_9 H + k_{10} H^{-2}}{1 + k_9 H_0 + k_{10} H_0^{-2}}$ $r_S = -k_3 r_X - k_6 X$ $r_P = k_4 r_X + k_7 X$ $r_H = k_{11} r_X$
9	Substrate limitation (Monod type) No substrate inhibition Ethanol inhibition (hyperbolic) Pirt's concept of substrate utilization Luedeking–Piret law Unrealistic asymptotic behaviour pH affected growth r_H proportional to r_X	k_1 to k_8 as in model 5 $k_9 = 2766$ $k_{10} = 1 \times 10^{-11}$ $k_{11} = 0.0023$	$r_X = \frac{k_1 XS}{k_2 F + S} \frac{1 - k_5 P}{1 + k_8 P}$ $F = \frac{1 + k_9 H + k_{10} H^{-2}}{1 + k_9 H_0 + k_{10} H_0^{-2}}$ $r_S = -k_3 r_X - k_6 X$ $r_P = k_4 r_X + k_7 X$ $r_H = k_{11} r_X$
10	Substrate limitation (Monod type) No substrate inhibition Ethanol inhibition (exponential) Herbert's concept of endogenous metabolism r_S proportional to $(r_X)_{growth}$ r_P proportional to $(r_X)_{growth}$ Realistic asymptotic behaviour pH affected growth r_H proportional to r_X	$k_1 = 0.3289$ $k_2 = 0.9645$ $k_3 = 12.93$ $k_4 = 5.705$ $k_5 = 0.0453$ $k_6 = 0.0288$ $k_9 = 10830$ $k_{10} = 6 \times 10^{-12}$ $k_{11} = 0.0023$	$(r_X)_{growth} = \frac{k_1 XS}{k_2 F + S} \exp(-k_5 P)$ $F = \frac{1 + k_9 H + k_{10} H^{-2}}{1 + k_9 H_0 - k_{10} H_0^{-2}}$ $(r_X)_{end} = -k_6 X$ $r_X = (r_X)_{growth} + (r_X)_{end}$ $r_S = -k_3 (r_X)_{growth}$ $r_P = k_4 (r_X)_{growth}$ $r_H = k_{11} r_X$

[a]Values valid if t is given in hours, X, S and P in g dm^{-3}, and H in mol dm^{-3}.

the process of ethanol fermentation. Figures 1–3 present a comparison of the relevant calculated and experimental data.

In model 3 the substrate consumption rate was described by the equation proposed by Pirt [28],

$$r_S = -k_3 r_X - k_6 X \tag{11}$$

whereas the ethanol formation rate was defined by the empirical Luedeking–Piret law [29]

$$r_P = k_4 r_X + k_7 X \tag{12}$$

Introduction of these changes resulted in a further improvement in the residual variance ($\sigma_R^2 = 0.0028$) and in a very good agreement between model predictions and experimental data (see Figs. 1–3).

The equation for biomass growth rate in model 4 additionally accounts for inhibition due to a high substrate concentration:

$$r_X = \frac{k_1 XS}{k_2 + S + k_8 S^2} \exp(-k_5 P) \tag{13}$$

The term describing the effect of high substrate concentration is identical with the expression derived from the general mechanism of competitive inhibition. The constant k_8 in eqn. (13) is then equal to the equilibrium constant of the following enzymatic reaction:

$$I + E \rightleftharpoons E\text{–}I$$

where E denotes the enzyme and I is the inhibitor (substrate) [28]. Obviously, the mechanistic constant k_8 should be positive and such a constraint was used when estimating the parameters. The numerical calculation led to k_8 approaching zero, whilst the other parameters achieved values very close to those obtained for model 3. On this basis, one can conclude that for sucrose concentrations lower than 200 g dm^{-3}, the phenomenon of competitive inhibition by a high substrate concentration has no remarkable effect on process kinetics.

In model 5 a different expression describing the inhibitory effect of ethanol on biomass growth rate was used:

$$r_X = \frac{k_1 XS}{k_2 + S} \frac{1 - k_5 P}{1 + k_8 P} \tag{14}$$

The above form was originally suggested by Sevely *et al.* [22]. Note that the term describing the effect

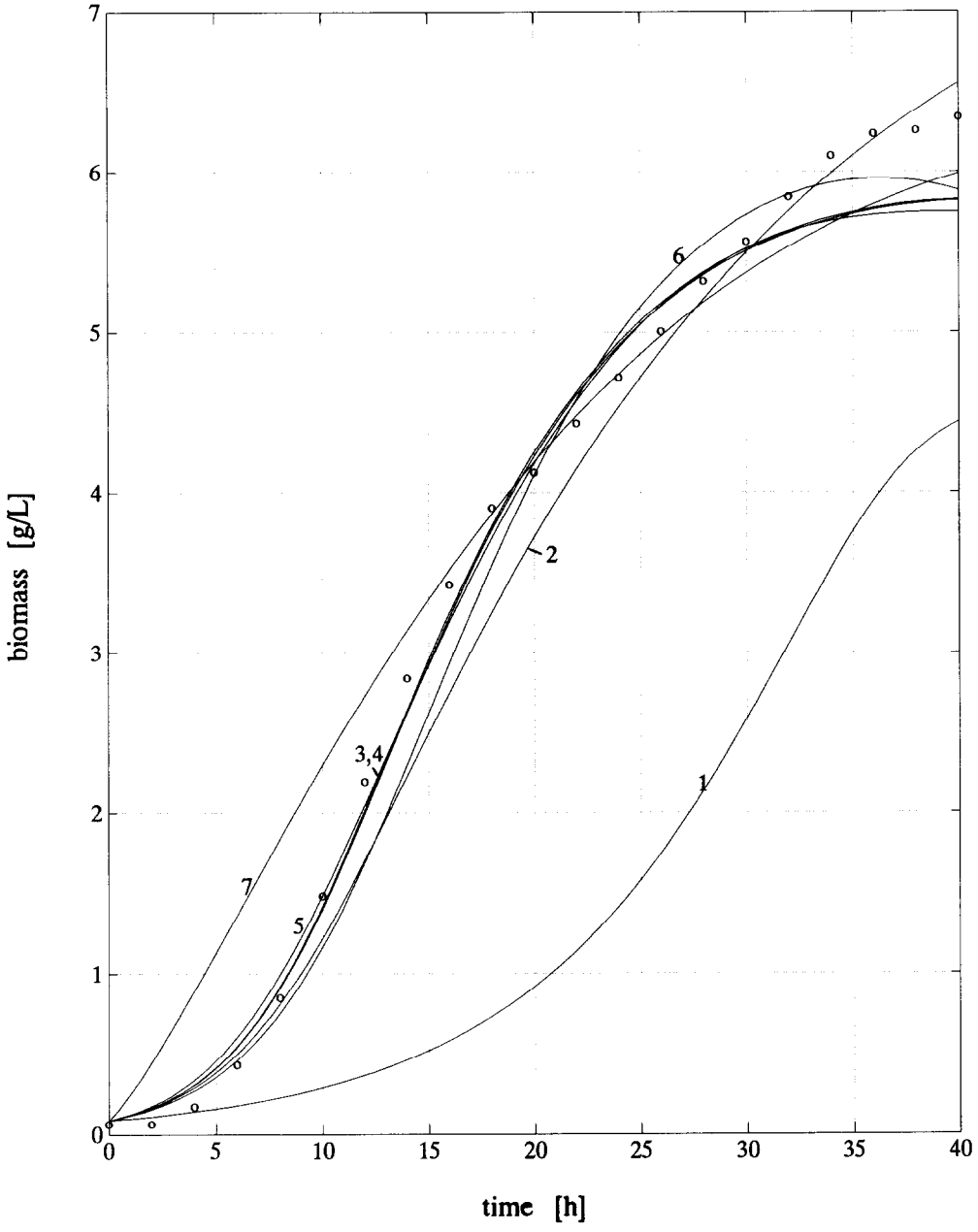

Fig. 1. Experimental and theoretical biomass concentrations at constant pH 5.8 (run 2); comparison of different kinetic models.

of product concentration on growth rate is analogous to the expression defining the effect of substrate concentration in the equation proposed by Kosaric *et al.* [10]. The results of computation are illustrated in Figs. 1–3. The model adequacy ($\sigma_R^2 = 0.0028$) is comparable with that obtained for model 3.

From the point of view of data fitting, models 3 and 5 can be considered accurate enough for a process duration not exceeding 40 h. In the case of longer fermentation times, the application of both models requires much care because of some disadvantageous asymptotic properties of the rate equations which lead to unrealistic concentration profiles when the substrate is being exhausted. Although both models predict the end of biomass growth at this point, they do not imply simultaneous decay of the rate of substrate consumption. Such a situation leads to negative concentrations of the substrate if the numerical simulation continues. Similar computational problems associated with this type of model were also reported by Roels [36].

The above disadvantage has been eliminated in model 6. This model was derived using assumptions substantially different from those presented so far.

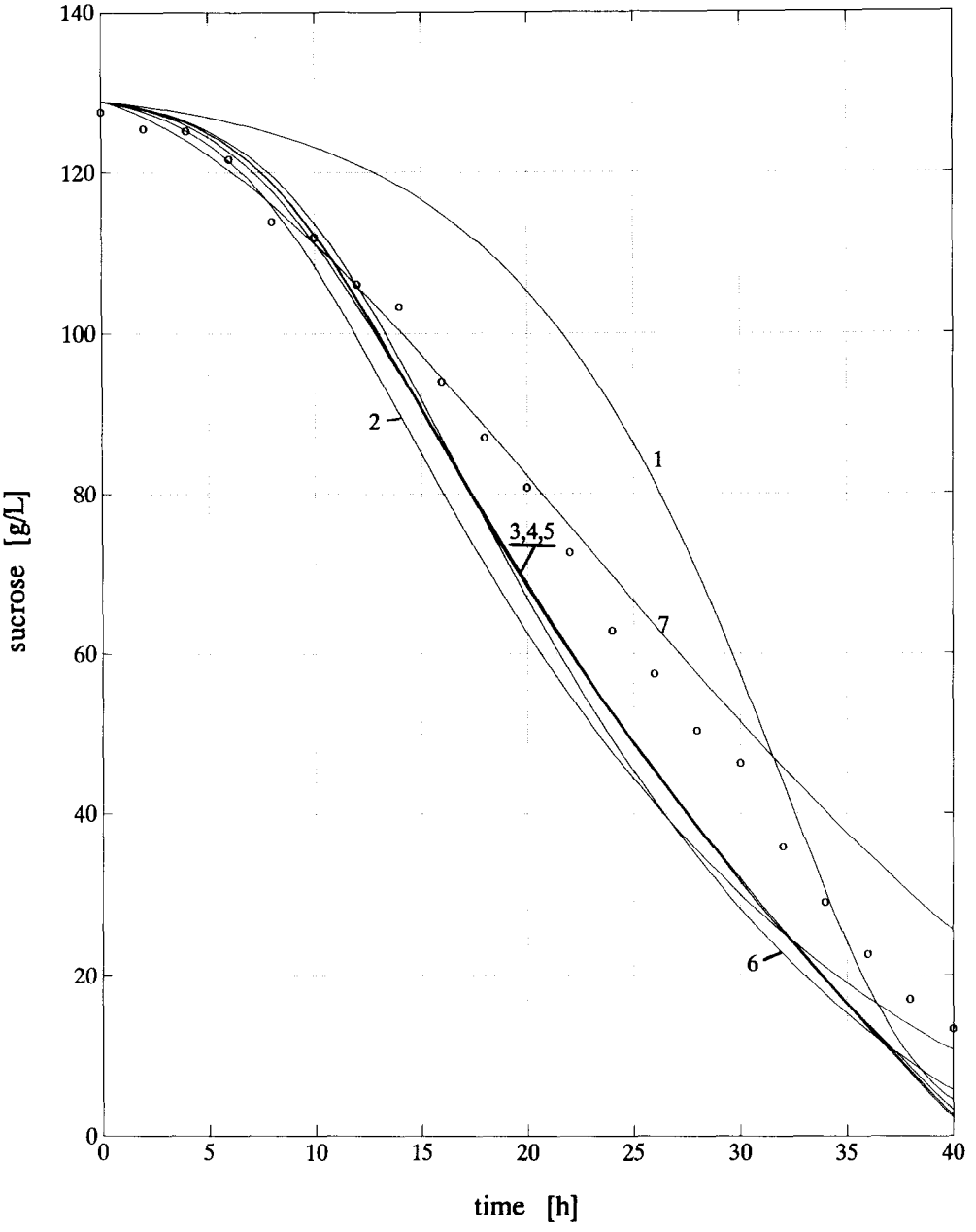

Fig. 2. Experimental and theoretical sucrose concentrations at constant pH 5.8 (run 2); comparison of different kinetic models.

According to Herbert's concept of growth [27], it was assumed that the gross (observed) rate of biomass formation comprised the growth rate and the rate of endogenous metabolism:

$$r_X = (r_X)_{growth} + (r_X)_{end} \quad (15)$$

For the growth rate, an expression involving the exponential product inhibition term, in the form of eqn. (13), was eventually accepted. Furthermore, it was assumed that the rates of substrate consumption and product formation are proportional to the biomass growth rate:

$$r_S = (r_S)_{growth} = -k_3(r_X)_{growth} \quad (16)$$

$$r_P = (r_P)_{growth} = k_4(r_X)_{growth} \quad (17)$$

The parameter k_3 in eqn. (16) is a reciprocal of the yield $Y_{X/S}$ associated with growth, while k_4 in eqn. (17) is equal to the stoichiometric coefficient $Y_{P/X}$ related to growth. The biomass growth rate was described by eqn. (10) and the rate of growth due to endogenous metabolism by a linear dependence:

$$(r_X)_{end} = -k_6 X \quad (18)$$

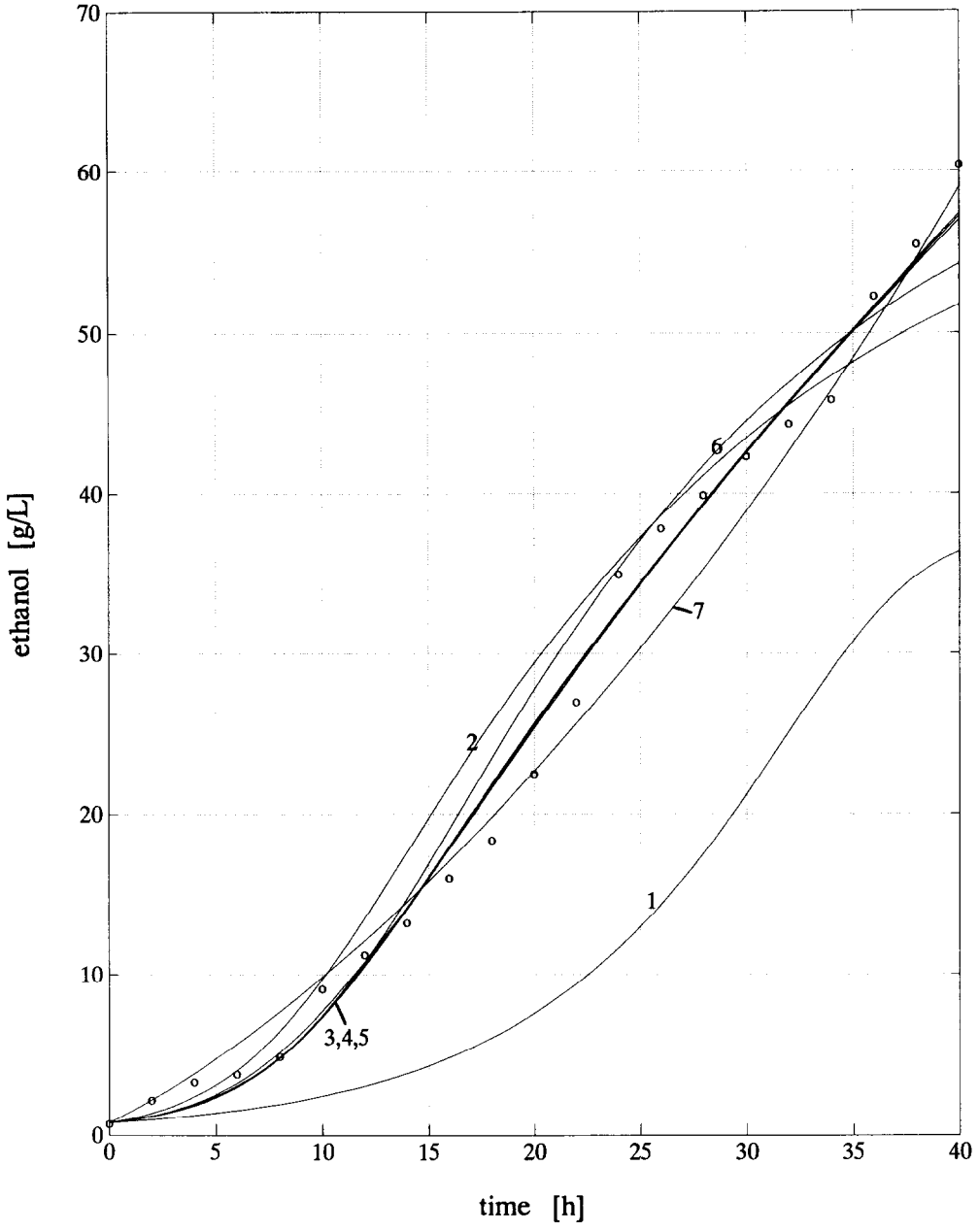

Fig. 3. Experimental and theoretical ethanol concentrations at constant pH 5.8 (run 2); comparison of different kinetic models.

The residual variance for this model was 0.0034, which is poorer than for models 3 and 5. However, the accuracy obtained (see Figs. 1–3) seems to be sufficient to recommend the model in practical applications.

Models 1–6 are examples of the classical approach to macromodelling of microbial kinetics. An alternative idea based on formal chemical kinetics, originally formulated for bioprocesses by Savageau and Voit [32], was employed in model 7. In this model, the kinetics of ethanol fermentation is represented schematically by the following diagram:

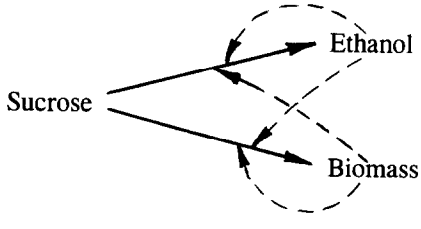

Solid lines represent the transport of species associated with elementary macrotransformations occurring in the system, and dashed lines denote either the activating or inhibiting effect of a given com-

ponent on individual reactions. The following equations can be deduced from the above diagram:

$$r_X = k_1 X^{k_2} S^{k_3} P^{k_4} \quad (19)$$

$$r_S = -k_5 X^{k_6} S^{k_7} P^{k_8} \quad (20)$$

$$r_P = k_9 X^{k_{10}} S^{k_{11}} P^{k_{12}} \quad (21)$$

Here, k_1, k_5 and k_9 are the apparent rate constants with positive values. The other constants are apparent reaction orders which can assume either positive (activation) or negative (inhibition) values. The value $\sigma_R^2 = 0.0027$ obtained for model 7 as well as the results of calculations presented in Figs. 1–3 are comparable with the results obtained for models 3–6. However, about half of the total error arose in this case from the biomass concentration while in the previous three models the error resulted mostly from poor fitting of the substrate concentration data (see Fig. 4). A serious drawback of model 7 is an excessive number of parameters to be evaluated which may make the reliability of the parameters obtained questionable. Moreover, the observed slow convergence (a very high number of iterations necessary to minimize the index $J(\boldsymbol{k})$) and the fact that the occurrence of local minima in the parameter space is very likely, make evaluation of the model parameters extremely time consuming. Application of this model to the simulation of complex ethanol fermentation systems may also evoke much numerical difficulty. Furthermore, a polynomial, and hence non-mechanistic and prominently approximative, form of the model practically excludes the possibility of its extrapolation beyond experimental conditions. However, it is worth noting that model 7 has no disadvantageous asymptotic properties which were revealed in the case of models 3–5. The discussion of the kinetic models applicable for constant pH conditions is summarized in Fig. 4 where contributions of individual species to the total residual variance σ_R^2 are shown. It may be concluded from this figure that Pirt's concept, although violating requirements for the proper asymptotic behaviour of fermentation, still gives the most satisfactory data fit for all three species assayed. In contrast, Herbert's concept enables one to simulate the asymptotic properties fairly well. Since it operates with a lower number of parameters (compared with Pirt's approach), the corresponding model is less flexible and leads to a slightly worse data fit.

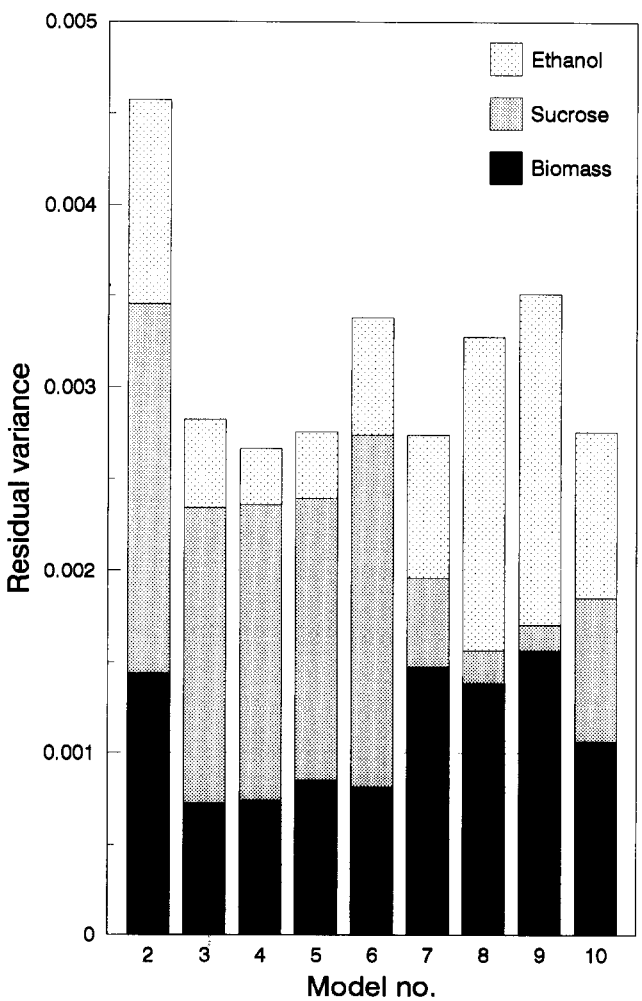

Fig. 4. Partition of residual variance σ_R^2 into biomass, sucrose and ethanol contributions for different kinetic models. Model 1 not shown (residual variance above 0.03).

4.2. *Models for uncontrolled pH conditions*

The hydrogen ion concentration has a significant effect on ethanol fermentation, particularly on the biomass growth rate. For models including the limitation of growth by substrate concentration, a quantitative approach to this problem can be represented by the equation

$$r_X = k_1 XS \Big/ \left[k_2 \left(1 + \frac{k_H}{k_{-H}} [H^+] + \frac{k_{OH}}{k_{-OH}} \frac{[OH^-]}{[H^+]} \right) + S \right] \quad (22)$$

where k_H, k_{-H}, k_{OH} and k_{-OH} are the rate constants of the following two reversible reactions [39]:

$$S + [H^+] \rightleftharpoons S\text{–}H^+$$

$$S + [OH^-] \rightleftharpoons S\text{–}OH^-$$

In this study, the above kinetic mechanism was verified using models 3 and 5 which represent Pirt's concept of substrate utilization. In order to adjust these models to varying pH conditions, the saturation

constant k_2 in growth rate equations was replaced by the product k_2F, where the pH-dependent correction factor F is defined according to eqn. (22) as follows:

$$F = \frac{1 + k_9 H + k_{10} H^{-2}}{1 + k_9 H_0 + k_{10} H_0^{-2}} \tag{23}$$

$H_0 = 10^{-5.8}$ mol dm^{-3} is the initial value of hydrogen ion concentration. Equation (23) has been normalized in such a way that for $H = H_0$, the factor F is unity and the product k_2F is identical with the constant k_2 in models 3 and 5.

Modelling of the fermentation process at varying pH should also include the rate of hydrogen ion formation r_H. This requires completion of the fermentor balance equations with the hydrogen ion balance equation:

$$\frac{dH}{dt} = r_H \qquad H(0) = H_0 \tag{24}$$

A systematic drop in pH level is observed experimentally when the fermentation proceeds, indicating that hydrogen ion formation is closely associated with microbial growth. In order to describe the rate of hydrogen ion formation in the simplest way, it was assumed proportional to the biomass growth rate:

$$r_H = k_{11} r_X \tag{25}$$

The revision of models 3 and 5 for conditions of varying pH resulted in models 8 and 9 respectively. In models 8 and 9 the parameters k_1 through k_8 were not estimated. Instead, these parameters were taken straight from models 3 and 5, and the estimation involved only the parameters of eqns. (23) and (25). Consequently, the calculations were performed using only the data collected at uncontrolled pH. Concentration profiles obtained on the basis of models 8 and 9 are shown in Figs. 5–7. The models yielded comparable results. A good agreement of model predictions with the experimental data ($\sigma_R^2 = 0.0033$ and $\sigma_R^2 = 0.0035$ respectively) confirms the validity of the employed assumptions about the influence of pH on process kinetics.

The Herbert concept of endogenous metabolism (model 6) was adjusted to varying pH conditions as well. The modification was carried out in the same way as previously for models 3 and 5. In the resulting model 10, the estimation procedure concerned all eight parameters of the model and involved the experimental data for both constant and varying pH. The requisite asymptotic behaviour of rate equations and an acceptable result of data fitting ($\sigma_R^2 = 0.0028$, see Figs. 5–7) appeared to make model 10 the most suitable for description of ethanol fermentation in the range of initial sucrose concentrations $S_0 = 130$–210 g dm^{-3} and pH 3–6.

Although the pH data were not used in the identification procedure, all three models properly predict the main trend in the observed pH behaviour giving a systematic decrease in pH from the initial value of 5.8 to about 2 in the late phase of the experiment (see Fig. 8). Also, an inspection of the F-factor curve, especially the location of its flat minimum, reveals a good agreement between the available literature data [40, 41] and the model predictions. Figure 9 shows the dependence of the F-factor on pH predicted by model 8. The minimum (corresponding to a maximum growth rate) lies within the expected range of pH 3.5–5.5.

4.3. *A biochemically structured model*

A common feature of all the models discussed so far is the avoidance of process stoichiometry. It is evident, however, that a more rational modelling of fermentation systems should also respect the most elementary stoichiometric relations which may impose important constraints on process rates. A careful and detailed analysis presented below for ethanol fermentation allowed such constraints to be determined.

One of the most important coefficients related to fermentation stoichiometry is the yield of product from the substrate $Y_{P/S}$. This coefficient can be defined at any moment of fermentation as the ratio of the product formation rate r_P and the substrate utilization rate $-r_S$:

$$Y_{P/S} = \frac{r_P}{-r_S} \tag{26}$$

As a result, in batch fermentations $Y_{P/S}$ is a time-dependent variable. However, in general, it is more convenient to consider $Y_{P/S}$ a function of the specific growth rate μ. An inspection of the list of metabolic pathways presented in Table 1 shows that reaction III is the only reaction in which ethanol is produced (the corresponding rate of ethanol formation $(r_P)_{III}$ is positive). In other reactions (II and IX) ethanol is consumed, so their contributions to the net ethanol formation rate r_P are negative. This means that

$$r_P < (r_P)_{III} \tag{27}$$

In turn, sucrose is mainly consumed in reaction III with the rate $(-r_S)_{III}$, and to a considerably lesser extent in some other reactions (I, IV–VIII). This means that the net rate of substrate utilization $-r_S$ must satisfy the inequality:

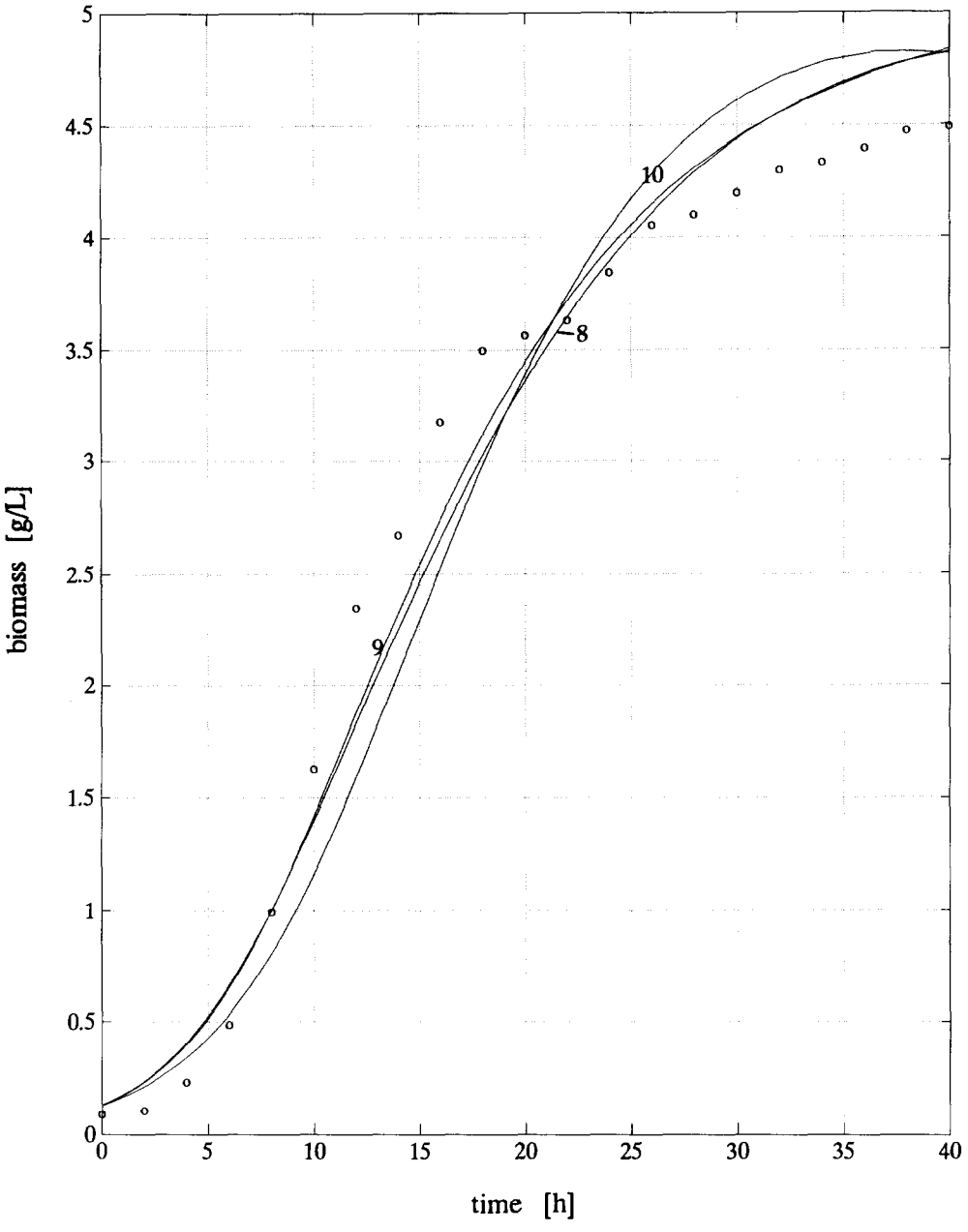

Fig. 5. Experimental and theoretical biomass concentrations under uncontrolled pH conditions (run 4); comparison of different kinetic models.

$$-r_S > (-r_S)_{III} \tag{28}$$

Now, it can be easily deduced that

$$Y_{P/S} = \frac{r_P}{-r_S} < \frac{(r_P)_{III}}{-r_S} < \frac{(r_P)_{III}}{(-r_S)_{III}} = (Y_{P/S})_{max} \tag{29}$$

where the maximum theoretical yield of ethanol from sucrose $(Y_{P/S})_{max}$ can be calculated from the stoichiometry of the leading reaction III as 0.53835 g ethanol per g sucrose consumed. Condition (29) means that the function $Y_{P/S}(\mu)$ is bounded, *i.e.*

$$Y_{P/S}(\mu) < (Y_{P/S})_{max} \tag{30}$$

The functional form of $Y_{P/S}(\mu)$ depends on the types of expression used for r_P and r_S. If we take r_P and r_S as mutually independent then the boundedness condition (30) may be violated. This can be illustrated by studying the behaviour of $Y_{P/S}(\mu)$ for several kinetic models of ethanol fermentation elaborated in the first part of the paper. Figure 10 shows that simple models of Monod type (models 1 and 2) as well as those based on Herbert's concept of endogenous metabolism (model 6) give constant

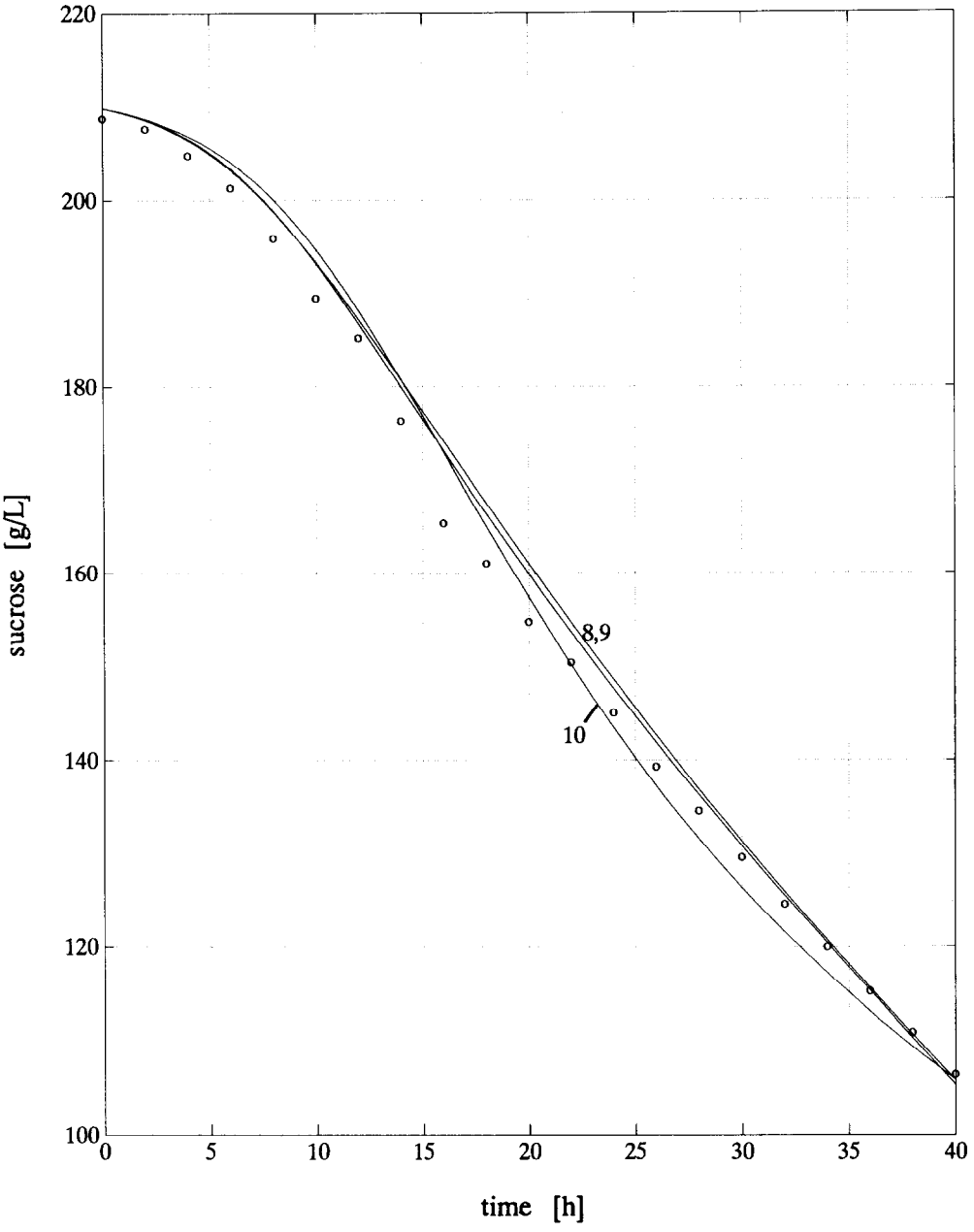

Fig. 6. Experimental and theoretical sucrose concentrations under uncontrolled pH conditions (run 4); comparison of different kinetic models.

values of $Y_{P/S}$ lying below the maximum value $(Y_{P/S})_{max}$. Other models give non-constant functions $Y_{P/S}(\mu)$. For the models supported by Pirt's concept of substrate utilization and the Luedeking–Piret law (models 3 and 5), values of $Y_{P/S}(\mu)$ range between 80% and 100% of $(Y_{P/S})_{max}$, while for model 7 based on formal kinetics, $Y_{P/S}(\mu)$ significantly exceeded $(Y_{P/S})_{max}$ for some μ. The above analysis proves that least-square identification of fermentation kinetics based on fitting concentration data with no additional parameter constraints may be insufficient to develop a relevant kinetic model satisfying elementary stoichiometric requirements. The missing constraints can be discovered, however, using the Roels idea of biochemically structured models [34–36].

The biochemically structured model of ethanol fermentation on sucrose can be constructed following the method originally applied by Roels to fermentation on glucose [36]. Considering reactions I, III and IV, XI and XII (Table 1) as predominant, it can be concluded from reaction stoichiometry that the net molar formation rates of individual

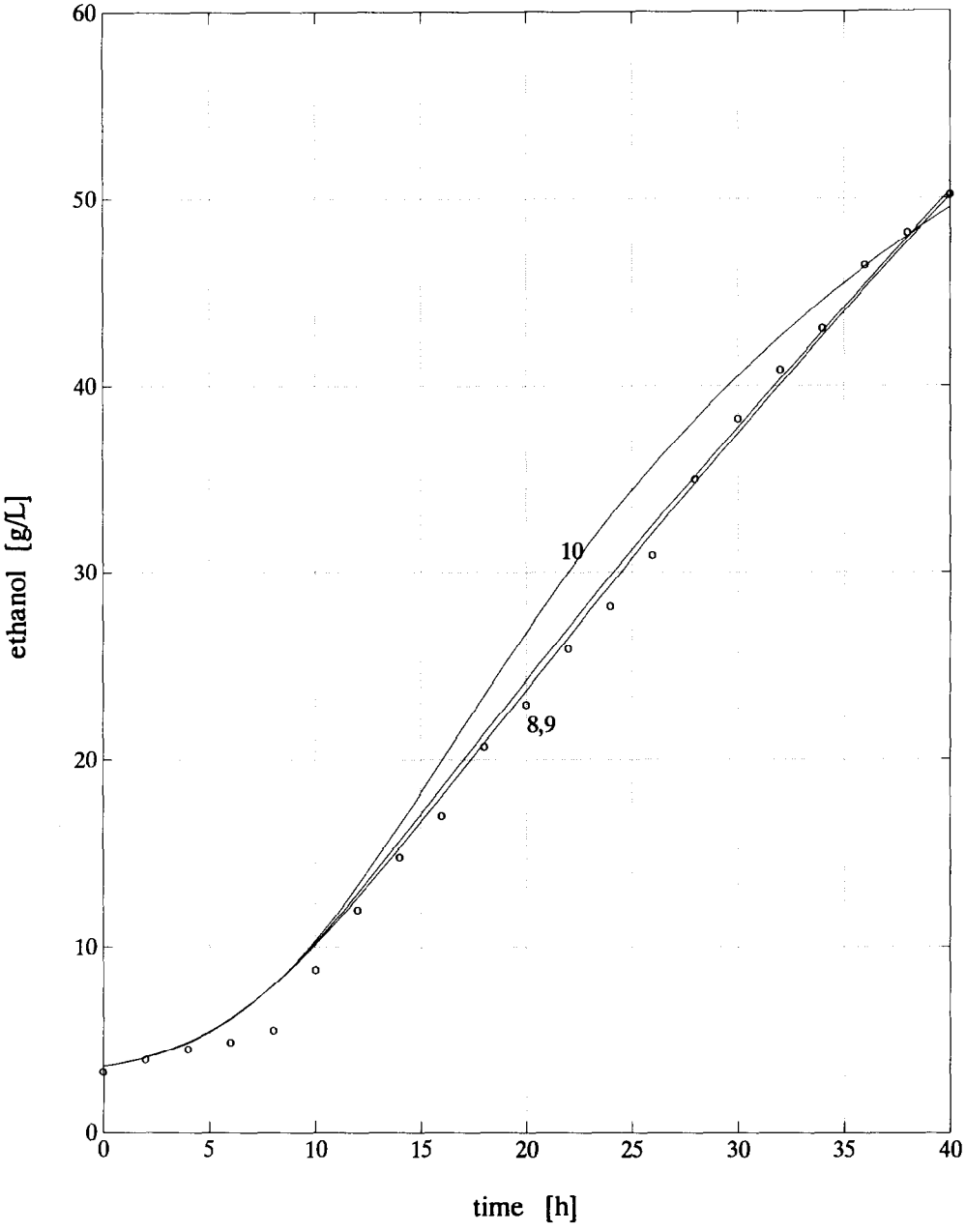

Fig. 7. Experimental and theoretical ethanol concentrations under uncontrolled pH conditions (run 4); comparison of different kinetic models.

species are

$$R_S = -1.095(R_{pre})_I - 1.5R_P - R_G \quad (31a)$$

$$R_{ATP} = -0.051(R_{pre})_I + 0.5R_P - (1/3)R_G + (R_{ATP})_{XI+XII} \quad (31b)$$

$$R_{H_2} = 0.13(R_{pre})_I - (1/3)R_G \quad (31c)$$

$$R_{pre} = (R_{pre})_I - R_X \quad (31d)$$

Roels *et al.* [34–36] applied the quasi-steady-state approximation (QSSA) to both intermediates of the reaction system, *i.e.* ATP and $NADH_2$. In fact, they used the QSSA for the biomass precursors too, although it was not shown explicitly in their papers. To be mathematically rigorous, however, the rate R_{pre} should also vanish at quasi-steady-state conditions. Finally, after employing the QSSA the above system of rate equations yields the following net molar rates of formation:

$$R_S = -2.028R_X + 3(R_{ATP})_{XI+XII} \quad (32a)$$

$$R_P = 0.362R_X - 2(R_{ATP})_{XI+XII} \quad (32b)$$

$$R_G = 0.39R_X \quad (32c)$$

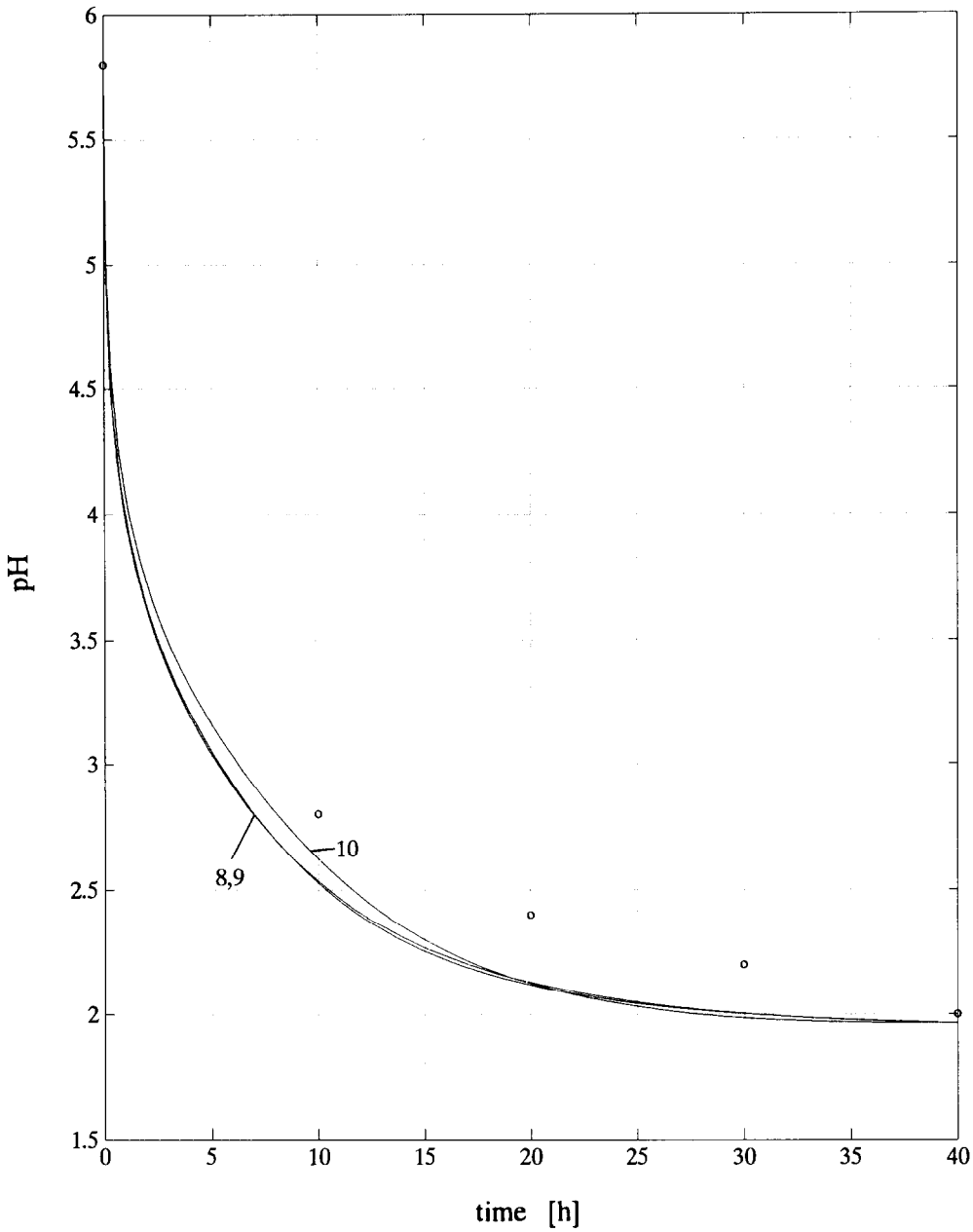

Fig. 8. Uncontrolled pH, run 4; pH profiles predicted by models 8, 9 and 10.

Thus, the above three formation rates are linearly dependent on the biomass growth rate R_X and the rate of ATP formation due to biomass precursor polymerization and maintenance $(R_{ATP})_{XI+XII}$.

On using appropriate experimental data Roels [36] found that

$$(R_{ATP})_{XI+XII} = -\kappa R_X - m_{ATP} c_X \quad (33)$$

with $\kappa = 2$ mol ATP per mol D.W. and $m_{ATP} = 0.05$ mol ATP per h mol D.W. This empirical rate equation can be incorporated easily into the kinetic model, giving final expressions for the net molar rate of substrate consumption and product formation as follows:

$$R_S = -8.03R_X - 0.15c_X \quad (34a)$$

$$R_P = 4.36R_X + 0.10c_X \quad (34b)$$

The molecular weight of biomass, $M_X = 26.1$ g per mol D.W., was estimated assuming an ash content of 8% D.W. Hence, equivalently, in terms of mass, one can obtain

$$r_S = -8.77r_X - 0.1637X \quad (35a)$$

$$r_P = 3.84r_X + 0.0881X \quad (35b)$$

$$r_G = 0.46r_X \quad (35c)$$

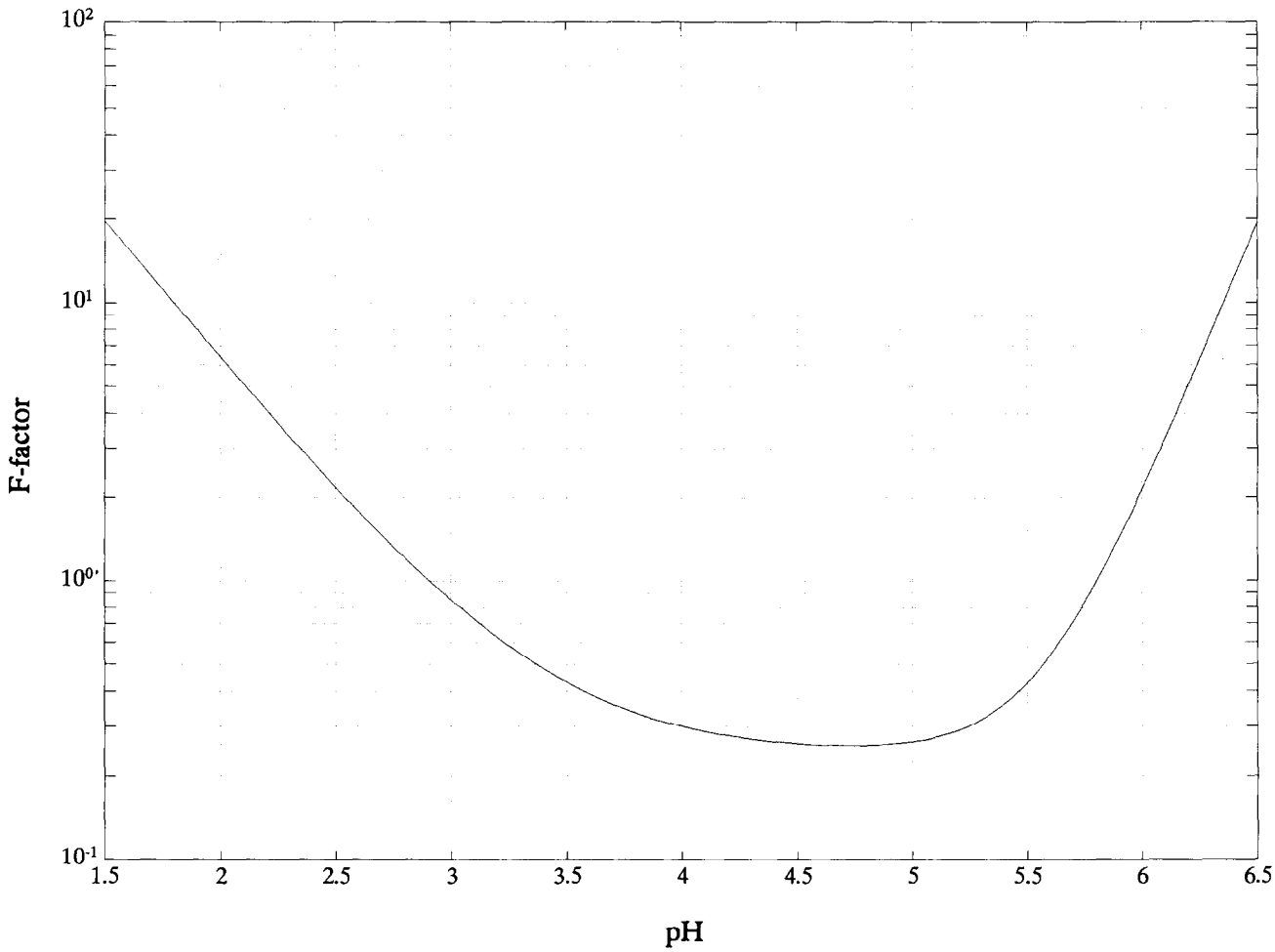

Fig. 9. Dependence of the F-factor on pH predicted by model 8.

The formation rates r_S and r_P determine the yield of ethanol as a function of the specific growth rate μ as follows:

$$Y_{P/S}(\mu) = \frac{3.84\mu + 0.0881}{8.77\mu + 0.1637} \tag{36}$$

The locus of $Y_{P/S}(\mu)$ for the Roels model of ethanol fermentation on sucrose has been plotted for $\mu > 0$ in Fig. 10. This figure shows that the model gives a yield function which is monotonically decreasing for positive μ, from the maximum value of $(Y_{P/S})_{max}$ at $\mu = 0$ to the minimum value of $0.813(Y_{P/S})_{max}$ when the variable μ tends to infinity (in fact, one should remember that μ is always less than the maximum specific growth rate μ_{max}). This monotonic behaviour of $Y_{P/S}(\mu)$ is an inseparable feature of the Roels model. Moreover, it can be shown easily that the monotonicity depends neither on the empirical constants κ and m_{ATP}, nor on the stoichiometric coefficients of reactions I, III and IV (see Appendix B).

Undoubtedly, the real (observed) yield function would differ slightly from the Roels theoretical model. However, it can be expected that the general mathematical form resulted from this approach, namely

$$Y_{P/S}(\mu) = \frac{k_4\mu + k_7}{k_3\mu + k_6} \tag{37}$$

would appear acceptable provided at least two constraints were imposed on parameters k_3, k_4, k_6 and k_7 (parameter notation as in models 3 and 5). The first constraint,

$$\frac{k_7}{k_6} < (Y_{P/S})_{max} \tag{38}$$

expresses the stoichiometric requirements, whereas the second constraint represents the monotonicity condition $dY_{P/S}/d\mu < 0$:

$$\frac{k_3}{k_4}\frac{k_7}{k_6} > 1 \tag{39}$$

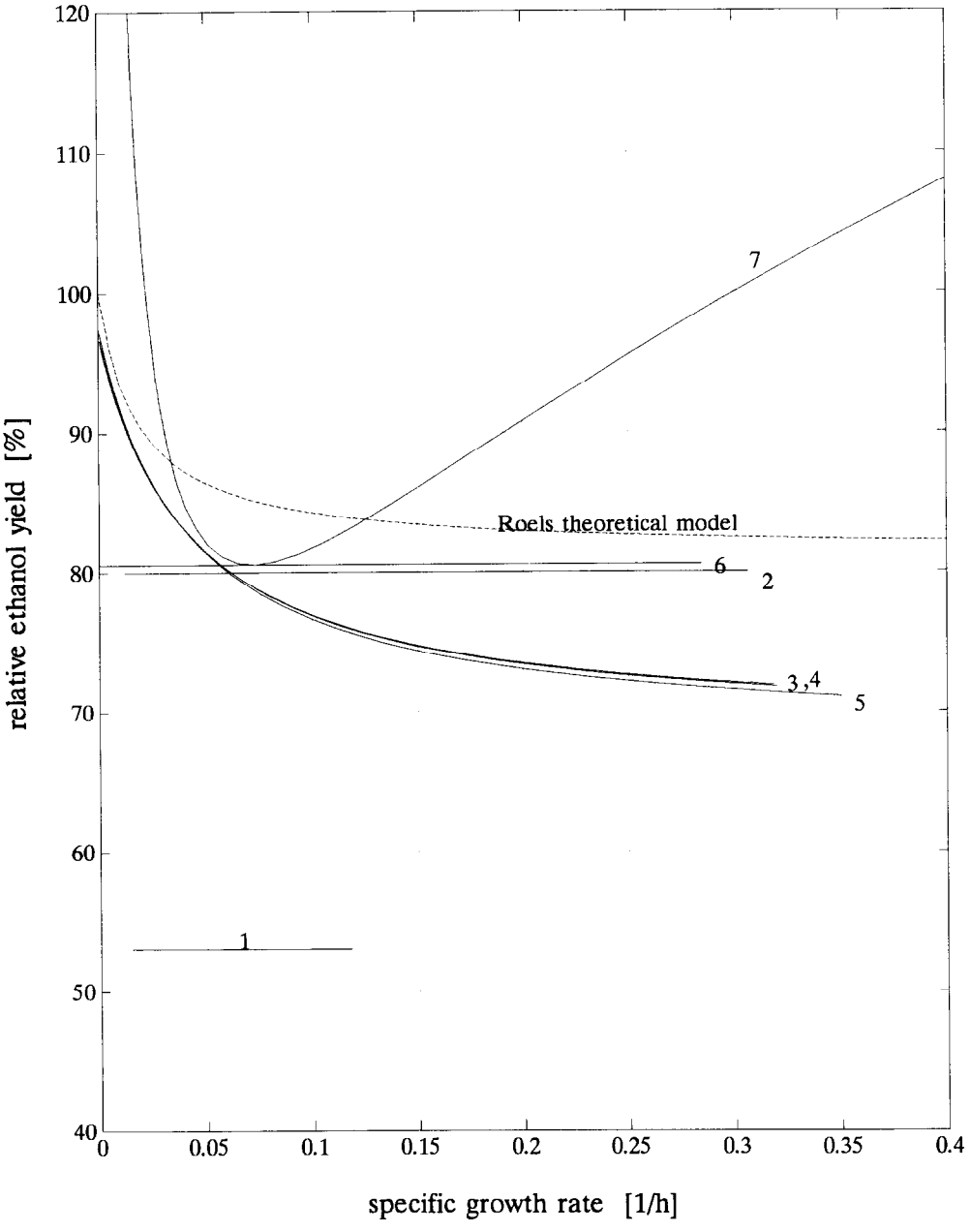

Fig. 10. Relative yield of ethanol from sucrose $[Y_{P/S}/(Y_{P/S})_{max}] \times 100\%$ *vs.* specific growth rate μ for the constant 5.8 pH fermentation, according to different kinetic models, results simulated for the conditions of run 2.

It is obvious now that the Roels model is a special case of model 3 (or 5) in which the above two parameter constraints have been used. Fortunately, the values of the parameters k_3, k_4, k_6 and k_7 obtained in the first part of this paper for both models 3 and 5 satisfy the conditions (38) and (39). Thus, the re-identification of these models with additional parameter constraints was not necessary.

5. Conclusions

Several kinetic models have been tested for quantification of the experimental batch data of ethanol fermentation both for constant and varying pH conditions (the list of models is shown in Table 3). Some of the models gave a satisfactory data fit over all measured concentrations. In the case of the best

fit models, the biomass growth rate was described by Monod type equations complemented by a term (exponential or hyperbolic) responsible for ethanol inhibition. Product inhibition has a very marked effect on process kinetics while the inhibition due to a high substrate concentration could be neglected for a sucrose concentration not exceeding 200 g dm^{-3}. The model based on Herbert's concept of growth rate (model 6) seems to be the most appropriate for bioengineering purposes in terms of practicality. The model involves a relatively small number of parameters and does not exhibit the disadvantageous asymptotic behaviour under conditions of substrate deprivation. Model 6 was also successfully adopted for varying pH conditions by including the equation for hydrogen ion formation rate and introducing a correction factor to the growth equation (model 10). Although the model based on the power-law formalism proposed by Savageau and Voit [32] (model 7) also yields a reasonably good fit to experimental data, it seems to be of limited applicability for modelling purposes because of certain computational problems involved.

Those models identified exclusively by fitting the concentration data might appear insufficient to satisfy elementary stoichiometric requirements. Such requirements, in the form of inequalities (38) and (39) imposed on some of the model parameters, have been developed using a biochemically structured model of ethanol fermentation.

References

1 A. Moser, in H. Bauer (ed.), *Biotechnology*, Vol. II, *Fundamentals of Biochemical Engineering*, Verlag Chemie, Weinheim, 1985, pp. 173–197.
2 J. Monod, *Recherches sur la Croissance des Cultures Bactériennes*, Hermann, Paris, 1942, 2nd edn.
3 N.D. Yerusalimskii, *Osnovi Fiziologii Mikrobov*, Isv. Akad. Nauk SSSR, Moscow, 1963.
4 M. Novak, P. Strehaiano, M. Moreno and G. Goma, *Biotech. Bioeng.*, *23* (1981) 201–211.
5 G.K. Hoppe and G.S. Hansford, *Biotechnol. Lett.*, *4* (1982) 39–44.
6 I. Holzberg, R.K. Finn and K.H. Steinkraus, *Biotech. Bioeng.*, *9* (1967) 413–427.
7 T.K. Ghose and R.D. Tyagi, *Biotech. Bioeng.*, *21* (1979) 1401–1420.
8 R.D. Tyagi and T.K. Ghose, *Biotech. Bioeng.*, *24* (1982) 781–795.
9 K.J. Lee and P.L. Rogers, *Chem. Eng. J. (Lausanne)*, *27* (1983) B31–B38.
10 N. Kosaric, S.L. Ong, Z. Duvnjak and A. Moser, *Acta Biotechnol.*, *4* (1984) 153–162.
11 A. Nipkow, B. Sonnleitner and A. Fiechter, *J. Biotechnol.*, *4* (1986) 35–47.
12 A.J. Daugulis and D.E. Swaine, *Biotech. Bioeng.*, *29* (1987) 639–645.
13 G.A. Hill and C.W. Robinson, *Chem. Eng. J. (Lausanne)*, *44* (1990) B69–B80.
14 J.M. Lee, J.F. Pollard and G.A. Coulman, *Biotech. Bioeng.*, *25* (1983) 497–511.
15 B.L. Maiorella, H.W. Blanch and C.R. Wilke, *Biotech. Bioeng.*, *26* (1984) 1003–1025.
16 J.H.T. Luong, *Biotech. Bioeng.*, *27* (1985) 280–285.
17 M.R. Melick, M.N. Karim, J.C. Linden, B.E. Dale and P. Mihaltz, *Biotech. Bioeng.*, *29* (1987) 370–382.
18 A.B. Jarzębski, J.J. Malinowski and G. Goma, *Biotech. Bioeng.*, *34* (1989) 1225–1230.
19 S. Aiba and M. Shoda, *J. Ferment. Technol.*, *47* (1969) 790–794.
20 C.K. Jin, H.L. Chiang and S.S. Wang, *Enzyme Microb. Technol.*, *3* (1981) 249–257.
21 T. Chattaway, G. Goma and P.-Y. Renaud, *Biotech. Bioeng.*, *32* (1988) 271–276.
22 Y. Sevely, J.P. Pourciel, G.R. Rauzy and J.P. Babans, paper presented at the *8th IFAC Triennial Congress, Kyoto, 1981.*
23 M. Nagatani, *J. Ferment. Technol.*, *51* (1973) 205–208.
24 A. Dourado, G. Goma, U. Albuquerque and Y. Sevely, *Biotech. Bioeng.*, *29* (1987) 187–194.
25 K. Richter, U. Becker and D. Meyer, *Acta Biotechnol.*, *9* (1989) 17–23.
26 K. Richter, U. Becker and D. Meyer, *Acta Biotechnol.*, *9* (1989) 25–33.
27 D. Herbert, in G. Tunevall (ed.), *Recent Progress in Microbiology*, Almquist and Wiksell, Stockholm, 1959, pp. 381–392.
28 S.J. Pirt, *Principles of Microbe and Cell Cultivation*, Blackwell Science Publishers, Oxford, 1975.
29 R. Luedeking and E.L. Piret, *J. Biochem. Microbiol. Technol. Eng.*, *1* (1959) 393–412.
30 A.S. Aiyar and R. Luedeking, *Chem. Eng. Progr., Symp. Ser.*, *62* (69) (1966) 55–59.
31 W. Borzani, M. Falcone and M.L.R. Vairo, *Appl. Microbiol.*, *8* (1960) 136–140.
32 M.A. Savageau and E.O. Voit, *J. Ferment. Technol.*, *60* (1982) 221–228.
33 J.P. Bovee, P. Strehaiano, G. Goma and Y. Sevely, *Biotech. Bioeng.*, *26* (1984) 328–334.
34 J.A. Roels, *Biotech. Bioeng.*, *22* (1980) 2457–2514.
35 J.G.J. Dekkers, H.E. de Kok and J.A. Roels, *Biotech. Bioeng.*, *23* (1981) 1023–1035.
36 J.A. Roels, *Energetics and Kinetics in Biotechnology*, Elsevier Biomedical, Amsterdam, 1983.
37 E. Oura, Reactions leading to the formation of yeast cell material from glucose and ethanol, *Report 8078*, 1972 (Alkon Keskuslaboratorio, Helsinki).
38 E. Oura, *Process Biochem.*, *12* (3) (1977) 19–21, 35.
39 L.N. Andreyeva and V.V. Biryukov, *Biotech. Bioeng. Symp.*, *4* (1973) 61–76.
40 N. Kosaric, A. Wieczorek, G.P. Cosentino, R.J. Magee and J.E. Prenosil, in H. Dellweg (ed.), *Biotechnology*, Vol. III, *Biomass, Microorganisms for Special Applications, Microbial Products: I, Energy from Renewable Resources*, Verlag Chemie, Weinheim, 1983, pp. 257–385.
41 B. Atkinson and F. Mavituna, *Biochemical Engineering and Biotechnology Handbook*, Macmillan, Surrey, 1983.
42 R.P. Jones and P.F. Greenfield, *Enzyme Microb. Technol.*, *4* (1982) 210–223.
43 S.L. Chen and F. Gutamis, *J. Gen. Microbiol.*, *118* (1980) 51–58.
44 J. Thibault, A. LeDuy and F. Côté, *Biotech. Bioeng.*, *30* (1987) 74–80.
45 J. Weiner, *J. Inst. Brew.*, *84* (1978) 222–223.

46 K. Levenberg, *Q. Appl. Math.*, *2* (1944) 164–168.
47 D.W. Marquardt, *J. SIAM*, *11* (1963) 431–441.
48 M. Nihtila and J. Virkkunen, *Biotech. Bioeng.*, *19* (1977) 1831–1850.
49 M. Nihtila, A program package for estimation of parameters in non-linear differential equation systems, *Report 7*, 1977 (Helsinki University of Technology, Control Engineering Laboratory, Helsinki).
50 J. Christiansen, *Numer. Math.*, *14* (1970) 317–324.

Appendix A: Nomenclature

c molar concentration (mol dm^{-3})
F factor accounting for variable pH, eqn. (23)
H hydrogen ion concentration (mol dm^{-3})
I number of experimental runs
J performance index
$\boldsymbol{k}$ vector of model parameters [k_1, k_2, .., k_p]
M molecular weight (g mol^{-1})
m maintenance coefficient (mol ATP per h mol D.W.)
N_i number of experimental points in ith run
n agitation speed (rev min^{-1})
P ethanol concentration (g dm^{-3})
p number of model parameters
R net molar rate of formation (mol dm^{-3} h^{-1})
r net mass rate of formation (g dm^{-3} h^{-1})
S sucrose concentration (g dm^{-3})
T temperature (K)
t time (h)
X biomass concentration (g dm^{-3})
$Y_{P/S}$ yield of ethanol from sucrose (g ethanol per g sucrose)
κ specific ATP demand for biomass polymerization (mol ATP per mol D.W.)
μ specific growth rate (h^{-1})
σ_R^2 total residual variance

Subscripts and superscripts
* experimental
G glycerol
H hydrogen ion
P product (ethanol)
S substrate (sucrose)
X biomass
0 initial
max maximum
pre biomass precursors

Appendix B

Let us recognize the following system of reactions as ethanol fermentation rate predominating (only sucrose, ethanol, glycerol, ATP, $NADH_2$, biomass precursors X_{pre} and biomass X have been taken into account in the process stoichiometry):

$$\alpha_{11}CH_{11/6}O_{11/12} + \alpha_{12}ATP \longrightarrow X_{pre} + \alpha_{13}'H_2'$$

$$\alpha_{21}CH_{11/6}O_{11/12} \longrightarrow CH_3O_{0.5} + \alpha_{22}ATP$$

$$\alpha_{31}CH_{11/6}O_{11/12} + \alpha_{32}ATP + \alpha_{33}'H_2' \longrightarrow CH_{8/3}O$$

$$X_{pre} + \kappa ATP \longrightarrow X$$

$$ATP \longrightarrow \text{Energy for maintenance}$$

where α_{ij} and κ are stoichiometric coefficients. The application of the QSSA with reference to ATP, $NADH_2$ and biomass precursors X_{pre} enables the determination of the elementary rates of formation:

$$R_S = -\alpha_{11}(R_{pre})_I - \alpha_{21}R_P - \alpha_{31}R_G \quad \text{(B1)}$$

$$R_{ATP} = -\alpha_{12}(R_{pre})_I + \alpha_{22}R_P - \alpha_{32}R_G - \kappa R_X - m_{ATP}c_X = 0 \quad \text{(B2)}$$

$$R_{H_2} = \alpha_{13}(R_{pre})_I - \alpha_{33}R_G = 0 \quad \text{(B3)}$$

$$R_{pre} = (R_{pre})_I - R_X = 0 \quad \text{(B4)}$$

and hence

$$R_S = -\left[\alpha_{11} + \frac{\alpha_{13}}{\alpha_{33}}\alpha_{31} + \frac{\alpha_{21}}{\alpha_{22}}\left(\alpha_{12} + \kappa + \frac{\alpha_{13}}{\alpha_{33}}\alpha_{32}\right)\right] \times R_X - \frac{\alpha_{21}}{\alpha_{22}}m_{ATP}c_X \quad \text{(B5)}$$

$$R_P = \left(\frac{\alpha_{12}+\kappa}{\alpha_{22}} + \frac{\alpha_{32}\alpha_{13}}{\alpha_{22}\alpha_{33}}\right)R_X + \frac{m_{ATP}}{\alpha_{22}}c_X \quad \text{(B6)}$$

According to the definition of ethanol yield from the substrate, given by eqn. (26), we have

$$Y_{P/S}(\mu) = \frac{a_1\mu + a_2}{b_1\mu + b_2}\frac{M_P}{M_S} \quad \text{(B7)}$$

where

$$a_1 = \alpha_{33}(\alpha_{12}+\kappa) + \alpha_{32}\alpha_{13} \quad \text{(B8)}$$

$$a_2 = \alpha_{33}m_{ATP} \quad \text{(B9)}$$

$$b_1 = \alpha_{11}\alpha_{22}\alpha_{33} + \alpha_{31}\alpha_{13}\alpha_{22} + \alpha_{33}\alpha_{21}(\alpha_{12}+\kappa) + \alpha_{21}\alpha_{32}\alpha_{13} \quad \text{(B10)}$$

$$b_2 = \alpha_{33}\alpha_{21}m_{ATP} \quad \text{(B11)}$$

Thus, the first derivative of $Y_{P/S}(\mu)$ is

$$\frac{dY_{P/S}}{d\mu} = \frac{\Delta}{(b_1\mu + b_2)^2}\frac{M_P}{M_S} \quad \text{(B12)}$$

where the discriminant

$$\Delta = a_1 b_2 - b_1 a_2 = -\alpha_{33}\alpha_{22}(\alpha_{11} + \alpha_{31})m_{ATP} < 0 \tag{B13}$$

turns out to be independent of μ. Inequality (B13) means that the yield function $Y_{P/S}(\mu)$ decreases monotonically regardless of the particular values of stoichiometric coefficients assumed. In other words, the monotonicity pattern found will be conserved for this model, even with different micro-organisms and carbon sources used, provided the essential metabolic pathways of the fermentation remain unchanged.